Influence of aerosols on the shortwave cloud radiative forcing from North Pacific oceanic clouds: Results from the Cloud Indirect Forcing Experiment (CIFEX)

Greg Roberts, Eric Wilcox, V. Ramanathan

Influence of aerosols on the shortwave cloud radiative forcing from North Pacific oceanic clouds: Results from the Cloud Indirect Forcing Experiment (CIFEX)

Eric M. Wilcox,[1] Greg Roberts,[2] and V. Ramanathan[2]

Received 8 June 2006; revised 24 August 2006; accepted 9 October 2006; published 3 November 2006.

[1] Aerosols over the Northeastern Pacific Ocean enhance the cloud drop number concentration and reduce the drop size for marine stratocumulus and cumulus clouds. These microphysical effects result in brighter clouds, as evidenced by a combination of aircraft and satellite observations. In-situ measurements from the Cloud Indirect Forcing Experiment (CIFEX) indicate that the mean cloud drop number concentration in low clouds over the polluted marine boundary layer is greater by 53 cm^{-3} compared to clean clouds, and the mean cloud drop effective radius is smaller by 4 μm. We link these in-situ measurements of cloud modification by aerosols, for the first time, with collocated satellite broadband radiative flux observations from the Clouds and the Earth's Radiant Energy System to show that these microphysical effects of aerosols enhance the top-of-atmosphere cooling by -9.9 ± 4.3 W m^{-2} for overcast conditions. **Citation:** Wilcox, E. M., G. Roberts, and V. Ramanathan (2006), Influence of aerosols on the shortwave cloud radiative forcing from North Pacific oceanic clouds: Results from the Cloud Indirect Forcing Experiment (CIFEX), *Geophys. Res. Lett.*, *33*, L21804, doi:10.1029/2006GL027150.

1. Introduction

[2] The albedo of low clouds will generally increase as the total liquid water path or geometric thickness of the cloud increases. For clouds of equivalent liquid water amount, however, anthropogenic aerosols acting as additional cloud condensation nuclei (CCN) are known to increase the albedo [*Twomey*, 1977; *Coakley et al.*, 1987]. Furthermore, suppression of drizzle may impact the liquid water path and the cloud fraction [*Albrecht*, 1989; *Ackerman et al.*, 2004]. The net radiative forcing of climate attributable to these indirect aerosol effects has been determined primarily using global atmospheric models, and the magnitude remains highly uncertain [*Lohmann and Feichter*, 2005]. This study reports on the influence of aerosol variations on shortwave cloud radiative forcing over the Northeast Pacific Ocean during April 2004 using observations from the Cloud Indirect Forcing Experiment (CIFEX). In-situ measurements document the aerosol influence on cloud microphysics, and satellite observations determine the resulting influence on cloud radiative forcing.

[3] CIFEX was conducted from April 1 to 21, 2004. During 24 flights in the U. of Wyoming King Air aircraft, a full complement of microphysical measurements were made including aerosol number concentration and size distribution (Particle Cavity Aerosol Spectrometer Probe; PCASP), and cloud drop number concentration and size distribution (Forward Scattering Spectrometer Probe; FSSP). Flights were conducted from Arcata, CA (41.0°N, 124.1°W) to approximately 650 km offshore, alternating between 5–10 min. aerosol sampling below cloud base and 5–10 min. cloud sampling below cloud top. Some clouds were profiled from cloud base to cloud top.

[4] Aerosols sampled during CIFEX have been classified based on the aerosol size distribution and back trajectories [*Roberts et al.*, 2006]. The aerosol types include North American aerosols, marine boundary layer aerosols, recently cloud-processed aerosols, and aerosols linked to Asian outflow. Within the Asian air masses, cases of recent new particle formation were found, as well as cases of aged aerosols. Aerosols linked to Asian outflow were found in layers above the boundary layer. Aerosol samples used in this study are limited to those in the boundary layer (below 1500 m). Most of the boundary layer aerosols encountered during CIFEX were composed of cloud-processed and North American continental aerosols.

[5] Cloud systems observed during CIFEX were predominantly stratocumulus and broken cumulus; some precipitating cumulus and mixed-phase clouds were also encountered. Under pristine conditions, low clouds were frequently observed to be drizzling.

[6] In this study we seek to document the impact of elevated concentrations of aerosol particles coincident with low clouds on the number concentration and size of cloud drops, as well as the resulting impact on shortwave cloud radiative forcing as determined by satellite albedo measurements from broadband radiometer observations. We advance a methodology that provides a quantitative measure of the enhanced shortwave cooling owing to the first aerosol indirect effect (the Twomey effect).

[7] Measurements of cloud drop number concentration (N_d), effective radius (r_{eff}) and albedo (α) are sorted according to the number concentration of aerosol particles (N_a) in the 0.1–3.0 μm diameter range as determined from the PCASP instrument, and evaluated as a function of cloud liquid water path (*LWP*) from the AMSR-E microwave radiometer on the Aqua satellite (F. Wentz and T. Meissner, AMSR-E/Aqua L2B Global Swath Ocean Products derived from Wentz Algorithm V001, March to June 2004, http://nsidc.org/data/ae_ocean.html). Albedo is observed from the Clouds and the Earth's Radiant Energy System (CERES) instrument [*Wielicki et al.*, 1996], which is also mounted on

[1] Laboratory for Atmospheres, NASA Goddard Space Flight Center, Greenbelt, Maryland, USA.
[2] Center for Atmospheric Sciences, Scripps Institution of Oceanography, University of California, San Diego, La Jolla, California, USA.

0094-8276/06/2006GL027150

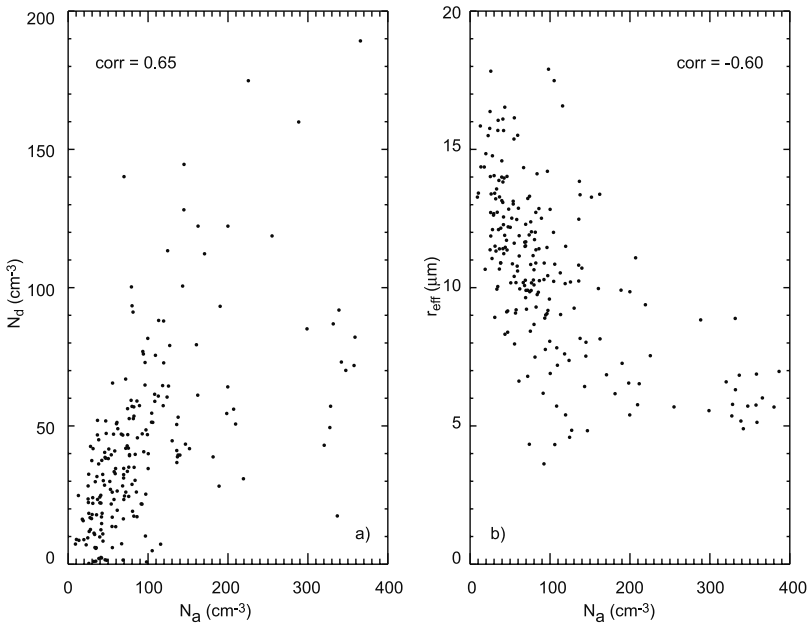

Figure 1. Scatter plots of aerosol number concentration (N_a) from aircraft PCASP (0.1–3.0 μm particle diameter) and (a) cloud drop number concentration (N_d); (b) cloud drop effective radius (r_{eff}) from aircraft FSSP measurements. Number of 0.25° grid cells is 218.

the Aqua satellite. Following the methodology of *Schwartz et al.* [2002] and *Peng et al.* [2002], cloud properties are evaluated for clouds of equivalent *LWP* to account for the strong dependence of cloud albedo on *LWP*, which varies primarily with cloud dynamics. Observations are taken from 11 flights on 9 different days. All aircraft and satellite data have been collocated in space by averaging over the same grid of 0.25° lat. by 0.25° lon. There is only one daytime pass of the Aqua satellite each day at approximately 1:30 pm local time. More than half of the aircraft data were collected within 3 hours before or after the corresponding afternoon overpass for the same day. A few aircraft samples may be as much as 6 hours apart from the corresponding Aqua overpass, which could introduce some error owing to evolving clouds. N_d and r_{eff} are averaged only over the cloudy samples in the grid cells, and N_a is averaged only over the clear-air samples in the grid cells. Cloudy air is distinguished from clear air in the in-situ data if there is a positive count in any of the FSSP, 1D-C, or 2D-C cloud probes. PCASP and FSSP observations are sampled at 1 s^{-1}. *LWP* is observed in 12 km AMSR-E footprints, and CERES α footprints are approximately 20 km at nadir. Only overcast values of *LWP* and α are used in the analysis. Overcast conditions within the AMSR-E and CERES footprints are determined using the 1 km Moderate Resolution Imaging Spectroradiometer (MODIS) cloud mask [*Ackerman et al.*, 1998]. Collocated MODIS cloud-top temperatures and cloud-phase retrievals were inspected to determine that the AMSR-E and CERES data were not influenced by high clouds above the clouds sampled by the aircraft.

2. Aerosol Impacts on Cloud Microphysics

[8] Polluted clouds are expected to have smaller drop sizes and higher drop concentrations compared to similar clean clouds. Figure 1 shows that, in general for clouds observed during CIFEX, N_d increases and r_{eff} decreases with increasing N_a. The FSSP probe has an estimated uncertainty of 14% for r_{eff} and 25% for N_d [*Baumgardner et al.*, 1992].

[9] To quantify the radiative forcing associated with the microphysical modification of clouds we compare the microphysical properties and albedos for clouds of the same *LWP*. The motivation for this approach is two-part. First, the clouds observed during CIFEX have *LWP* quantities ranging from 20 to 500 g m^{-2}. In this range of *LWP* values, the cloud albedo increases strongly with increasing *LWP* from 0.2 to 0.5 (Figure 4 in section 3). The *LWP* of low clouds is determined primarily by the temperature, humidity, and turbulence in the cloud environment. *Schwartz et al.* [2002] find that more than 83% of the variance in the optical depth of low clouds over the Atlantic Ocean is attributable to the variance in *LWP*. They conclude that because of the high variance in *LWP*, it is necessary to compare the albedos of clouds of the same *LWP* in order determine the aerosol influence on the albedo. Second, in the absence of entrainment or precipitation, cloud profiles will be roughly adiabatic [*Brenguier*, 1991]. Under this model there is a monotonic increase in *LWP* with cloud thickness. Liquid water content (*LWC*) and r_{eff} increase monotonically with height within the cloud, and N_d is constant with height. Thus, for adiabatic clouds of the same *LWP* we would expect to see the effects of aerosols in the microphysical properties of the observed clouds. Figure 2 shows the probability densities of the ratio of observed *LWC* to LWC_{adiab}, the expected adiabatic *LWC* computed according to *Brenguier* [1991], for four clean and three polluted clouds profiled during CIFEX on three different days (polluted is $N_a > 50$ cm^{-3} below cloud base). Similar to the results from ACE-2 clouds [*Brenguier et al.*, 2000], the densities peak at sub-adiabatic values, mostly associated with entrainment close to cloud top, although considerable scatter in the estimated ratio may also result from drizzle in some of the clean clouds. Furthermore, the flight tracks

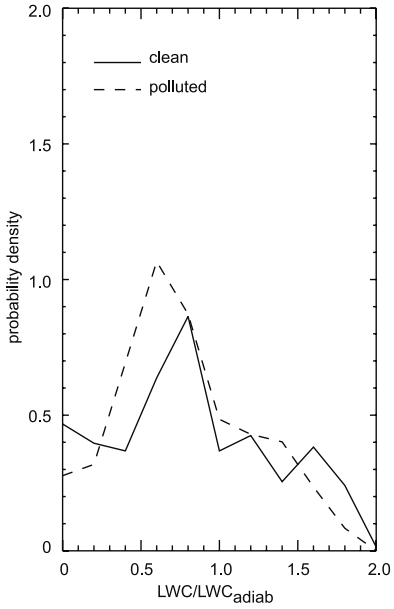

Figure 2. Probability density of the ratio of liquid water content to the adiabatic liquid water content within 4 clean and 3 polluted clouds profiled on days 4/3, 4/7, and 4/21.

were typically diagonal traverses through the clouds where the horizontal distance traveled from cloud base to cloud top may have been broader than the horizontal scale of individual clouds, which will introduce some error in the estimate of LWC/LWC_{adiab}, and may be the cause of the apparent super-adiabatic cases. The general sub-adiabaticity of the clouds is a source of error in comparing clouds of equivalent *LWP*, however we note that the probability densities for clean and polluted clouds are similar. Furthermore, it has been proposed that the LWP in stratocumulus clouds may increase with aerosol amount in some cases, and decrease with aerosols in other cases [e.g., *Han et al.*, 1998; *Albrecht*, 1989; *Ackerman et al.*, 2004].

[10] N_d and r_{eff} measured by the FSSP instrument are shown as functions of overcast *LWP* in Figure 3. Each data point is an average of observations falling within *LWP* bins of equal width along the logarithmic *LWP* scale. The vertical bars on each point are an estimate of the 95% confidence limit of the mean of all 0.25° grid cells in the *LWP* bin. The data have been further stratified into clean and polluted classes, defined as average N_a less than or greater than 50 cm^{-3}, respectively. N_a averages are restricted to samples at or below 1500 m altitude. Because the aircraft flight tracks typically alternated between level flight in the cloud layer and level flight below the cloud layer, the N_a averages largely comprise samples below cloud, and in some cases between clouds. The 50 cm^{-3} threshold corresponds to the average aerosol concentrations (diameter > 0.1 μm) for cloud processed airmasses in which most pollution has presumably been removed. Approximately one-third of all samples (including partly cloudy scenes) fall into the clean class and two-thirds into the polluted class. The median value of N_a is 70 cm^{-3}. The PCASP-100X probe has an estimated uncertainty of 10% for measurements of N_a. Only data where clear air N_a observations and cloudy air N_d observations coincide in the same grid cell are included. 93% of grid cells containing a cloudy air sample also contained a clear air aerosol sample, owing to the aircraft sampling pattern and the horizontal scales of the clouds.

[11] For clouds of equivalent liquid water path, the one associated with higher aerosol concentration will exhibit a larger N_d and smaller r_{eff} if the additional aerosols have enhanced the number of CCN. This is the case for clouds observed during CIFEX. N_d is greater and r_{eff} is smaller in the clouds classified as polluted compared to the clean clouds in all but the lowest *LWP* bin (Figure 3). Averages of N_d and r_{eff} are given in Table 1. r_{eff} is nearly 4 μm smaller

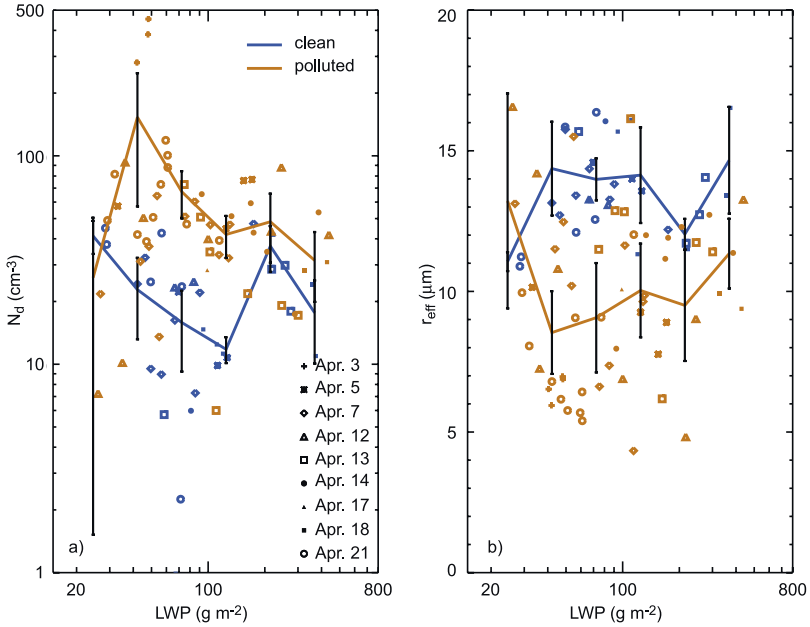

Figure 3. (a) Cloud drop number concentration (N_d), and (b) cloud drop effective radius (r_{eff}) from aircraft FSSP measurements. Both are shown as functions of cloud liquid water path (*LWP*) for clean and polluted clouds. Number of 0.25° grid cells is 113, comprising 17,748 1 s FSSP samples.

Table 1. Mean Microphysical Properties and Cloud Cover by Aerosol Concentration Classification

	Aerosol Number Conc. (0.1–3 μm diameter), N_a cm^{-3}	Cloud drop Number Conc., N_d cm^{-3}	Cloud Drop Effective Radius, r_{eff} μm
Clean	33	21	13.7
Polluted	124	74	9.7
Average	90	55	11.1

in the polluted clouds compared to the clean clouds, and N_d is more than 50 cm^{-3} greater in the polluted clouds. The difference between clean and polluted clouds is greatest for clouds with *LWP* between 30 and 110 g m^{-2}, comprising more than 80% of the clouds sampled.

3. Aerosol Effects on Shortwave Cloud Radiative Forcing

[12] The CERES instrument on-board the Aqua satellite measures reflected solar radiance in the 0.3 to 5 μm spectral range [*Wielicki et al.*, 1996]. MODIS imager observations within each CERES footprint characterize scene-specific angular distribution models which are used to convert the radiances to estimates of the radiative flux [*Loeb et al.*, 2005]. Uncertainty in the instantaneous shortwave flux at the top-of-atmosphere for cloudy-sky midlatitude scenes is estimated to be approximately 4%, and does not vary significantly with cloud optical depth or cloud fraction in liquid water clouds [*Loeb et al.*, 2003]. Shortwave cloud radiative forcing at the top of the atmosphere for diurnal mean insolation (C_{sm}) is determined from these observations. It is defined as the product of the diurnal mean insolation (S_o) and the difference between the clear-sky albedo (α_{clr}) and the cloud albedo (α):

$$C_{sm} = S_o(\alpha_{clr} - \alpha). \quad (1)$$

α_{clr} is evaluated for each satellite pass over the CIFEX region and is taken as the average albedo from cloud-free CERES ocean pixels in the region. In estimating C_{sm}, α is the CERES observed albedo for overcast footprints only. Partly cloudy footprints are excluded from the analysis in order to distinguish differences in albedo owing to differences in aerosol from those owing to differences in fractional cloud cover. We report the diurnal mean C_{sm} instead of the instantaneous shortwave radiative forcing (C_s) in order to estimate the magnitude of forcing by the first aerosol indirect effect under average conditions for clouds in the CIFEX region during April. Note, however that Aqua passes over the region only once each day at the same local time, therefore these results do not account for diurnal variations in cloud properties or variations in cloud albedo with solar zenith angle.

[13] Albedo and C_{sm} are shown as functions of *LWP* for the clean and polluted samples in Figure 4, where *LWP* averages are again limited to only overcast AMSR-E pixels. Radiative cooling by polluted clouds is greater than that of clean clouds in the 30 to 110 g m^{-2} *LWP* range where the increase in N_d and decrease in r_{eff} are most pronounced. Averages of C_{sm}, *LWP* and other quantities are summarized in Table 2. The average value of C_{sm} for all overcast samples is -110.3 W m^{-2}, and the averages for clean and polluted clouds are -103.9 W m^{-2} and -113.6 W m^{-2} respectively. *LWP* is lower by about 4% for the overcast polluted scenes compared to the clean scenes, which is within the uncertainty of the AMSR-E observations.

[14] To evaluate the enhancement of shortwave cloud radiative forcing owing to the greater concentration of smaller drops in the polluted clouds, we define a quantity C^c_{sm}:

$$C^c_{sm} = S_o(\alpha_{clr} - \alpha_{clean}) \quad (2)$$

where all samples in each *LWP* bin are assigned the average albedo for clean clouds in that bin. The resulting C^c_{sm} is an estimate of what the mean forcing for overcast conditions would be if N_a were always less than 50 cm^{-3}, and holding

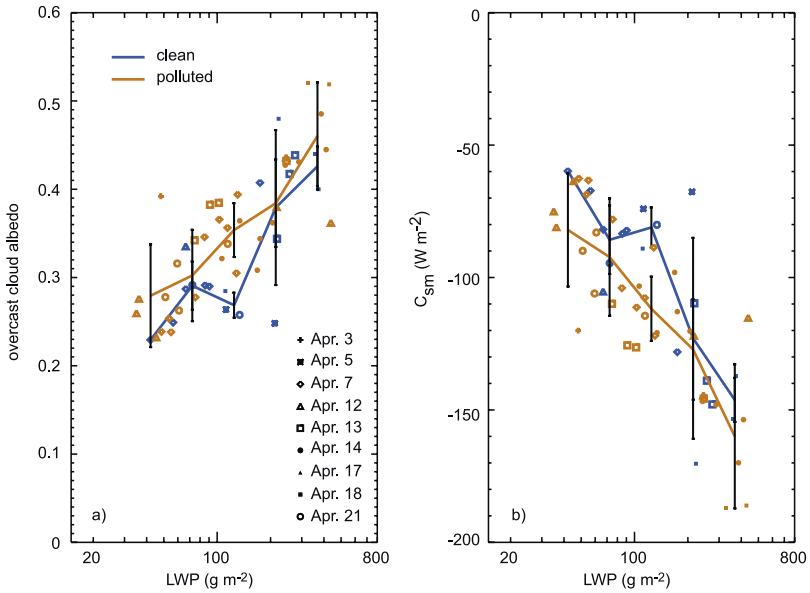

Figure 4. (a) Albedo (α), and (b) diurnal mean shortwave cloud radiative forcing (C_{sm}) for overcast CERES footprints. Both are shown as functions of cloud liquid water path (*LWP*) for clean and polluted clouds. Number of 0.25° grid cells is 53.

Table 2. Cloud Properties and Shortwave Cloud Radiative Forcing for Average, Clean, and Polluted Overcast Scenes[a]

	Ave.	Clean	Polluted
Num. of samples		18	35
C_{sm} (±4 W m^{-2})	−110.3	−103.9	−113.6
N_a (±9 cm^{-3})	89.9	34.0	118.6
LWP (±17 g m^{-2})	159.4	162.4	157.9
C_{sm}^c (±4 W m^{-2})	−100.4		
$C_{sm} - C_{sm}^c$ (±4 W m^{-2})	−9.9		
$C_{sm} - C_{sm}$(*clean*) (±4 W m^{-2})	−6.4		

[a]Uncertainties are published estimates of RMS error.

LWP unchanged. This quantity is subtracted from the mean C_{sm} for all clouds. The difference, $C_{sm} - C_{sm}^c$, is then a measure of the forcing by the first aerosol indirect effect for constant *LWP*. This quantity is -9.9 ± 4.3 W m^{-2} for the low clouds observed during CIFEX. The uncertainty is the standard deviation of the mean albedos in *LWP* bins and is consistent with the 4% uncertainty in the CERES angular distribution model reported by the CERES science team. The magnitude of the estimated shortwave cooling does depend on the choice of threshold N_a defining polluted clouds. If 70 cm^{-3} is used (the median value) instead of 50 cm^{-3}, then the magnitude of $C_{sm} - C_{sm}^c$ is reduced to −7.6 W m^{-2}.

[15] As already noted, the assumption that *LWP* remains constant under the influence of aerosols may not be strictly correct. Nevertheless, *LWP* will vary significantly among cloud cases owing to differences in the temperature, humidity, and turbulence within the cloud environment. Because the cloud albedo increases substantially with *LWP* it is necessary to take into account the *LWP* differences when comparing the albedos of clouds under different aerosol conditions [*Schwartz et al.*, 2002]. While we cannot determine the source of the *LWP* difference between the clean and polluted clouds (i.e., aerosols or cloud dynamics), the difference does reduce the cooling attributable to the Twomey effect under constant *LWP* estimated above. The difference between the mean cloud forcing and the cloud forcing averaged over the clean cloud samples only ($C_{sm} - C_{sm}$[*clean*] in Table 2) provides an estimate of the forcing including the *LWP* differences between clean and polluted clouds. This quantity is −6.4 W m^{-2}.

4. Conclusion

[16] The microphysical modification of low clouds by pollution in the marine boundary layer is shown to result in enhanced shortwave cooling at the top of the atmosphere in collocated satellite observations of broadband shortwave flux. Observations of low stratocumulus and cumulus clouds over the Northeast Pacific Ocean during April 2004 from the Cloud Indirect Forcing Experiment (CIFEX) indicate that N_d is greater by 53 cm^{-3} in clouds associated with aerosol number concentrations in the marine boundary layer greater than 50 cm^{-3} (for particles larger than 0.1 μm) compared with clean clouds associated with lower aerosol amounts. Cloud drop effective radius is smaller by 4 μm in polluted clouds compared with clean clouds. We show that by sorting the observed clouds by *LWP* measured with AMSR-E, these microphysical effects of aerosols can be related directly to an observed cooling at the top of the atmosphere using CERES broadband shortwave radiative flux data. Top-of-atmosphere cooling owing to the Twomey effect is -9.9 ± 4.3 W m^{-2} for overcast conditions.

[17] **Acknowledgments.** Guillaume Mauger, Odelle Hadley, John Holocek (UCSD), and Carl Schmidt (NCAR) contributed to the planning and execution of CIFEX. We are also grateful for efforts of the U. of Wyoming King Air crew. CERES data were obtained from the NASA Langley Research Center DAAC. CIFEX was funded by the National Science Foundation. The lead author was supported by a fellowship from the NOAA Postdoctoral Program in Climate and Global Change administered by the University Corporation for Atmospheric Research. AMSR-E data were obtained from the National Snow and Ice Data Center.

References

Ackerman, S. A., K. I. Strabala, W. P. Menzel, R. A. Frey, C. C. Moeller, and L. E. Gumley (1998), Discriminating clear-sky from clouds with MODIS, *J. Geophys. Res.*, *103*, 32,141–32,158.

Ackerman, A. S., M. P. Kirkpatrick, D. E. Stevens, and O. B. Toon (2004), The impact of humidity above stratiform clouds on indirect aerosol climate forcing, *Nature*, *432*, 1014–1017.

Albrecht, B. A. (1989), Aerosols, cloud microphysics, and fractional cloudiness, *Science*, *245*, 1227–1230.

Baumgardner, D., J. E. Dye, B. W. Gandrud, and R. G. Knollenberg (1992), Interpretation of measurements made by the Forward Scattering Spectrometer Probe (FSSP-300) during the Airborne Arctic Stratospheric Expedition, *J. Geophys. Res.*, *97*, 8035–8046.

Brenguier, J.-L. (1991), Parameterization of the condensation process: A theoretical approach, *J. Atmos. Sci.*, *48*, 264–282.

Brenguier, J.-L., H. Pawlowska, L. Schüller, R. Preusker, J. Fischer, and Y. Fouquart (2000), Radiative properties of boundary layer clouds: Droplet effective radius versus number concentration, *J. Atmos. Sci.*, *57*, 803–821.

Coakley, J. A., Jr., R. L. Bernstein, and P. A. Durkee (1987), Effect of ship-stack effluents on cloud reflectivity, *Science*, *237*, 1020–1022.

Han, Q., W. B. Rossow, J. Chou, and R. Welch (1998), Global survey of the relationships of cloud albedo and liquid water path with droplet size using ISCCP, *J. Clim.*, *11*, 1516–1528.

Loeb, N. G., et al. (2003), Angular distribution models for top-of-atmosphere radiative flux estimation from the Clouds and the Earth's Radiant Energy System instrument on the Tropical Rainfall Measuring Mission satellite: Part II. Validation, *J. Appl. Meteorol.*, *42*, 1748–1768.

Loeb, N. G., S. Kato, K. Loukachine, and N. Manalo-Smith (2005), Angular distribution models for top-of-atmosphere radiative flux estimation from the Clouds and the Earth's Radiant Energy System instrument on the Terra satellite: Part I. Methodology, *J. Atmos. Oceanic Technol.*, *22*, 338–350.

Lohmann, U., and J. Feichter (2005), Global aerosol indirect effects: A review, *Atmos. Chem. Phys.*, *5*, 715–737.

Peng, Y., U. Lohmann, R. Leaitch, C. Banic, and M. Couture (2002), The cloud albedo-cloud droplet effective radius relationship for clean and polluted clouds from RACE and FIRE. ACE, *J. Geophys. Res.*, *107*(D11), 4106, doi:10.1029/2000JD000281.

Roberts, G., G. Mauger, O. Lariviere, and V. Ramanathan (2006), North American and Asian aerosols over the eastern Pacific Ocean and their role in regulating cloud condensation nuclei, *J. Geophys. Res.*, *111*, D13205, doi:10.1029/2005JD006661.

Schwartz, S. E., Harshvardhan, and C. M. Benkovitz (2002), Influence of anthropogenic aerosol on cloud optical depth and albedo shown by satellite measurements and chemical transport modeling, *Proc. Natl. Acad. Sci.*, *99*, 1784–1789.

Twomey, S. (1977), The influence of pollution on the shortwave albedo of clouds, *J. Atmos. Sci.*, *34*, 1149–1152.

Wielicki, B. A., B. R. Barkstrom, E. F. Harrison, R. B. Lee III, G. L. Smith, and J. E. Cooper (1996), Clouds and the Earth's Radiant Energy System (CERES): An Earth observing system experiment, *Bull. Am. Meteorol. Soc.*, *77*, 853–868.

V. Ramanathan and G. Roberts, Center for Atmospheric Sciences, Scripps Institution of Oceanography, University of California, 9500 Gilman Drive, La Jolla, CA 92093, USA.

E. Wilcox, NASA Goddard Space Flight Center, Code 613.2, Greenbelt, MD 20771, USA. (eric.m.wilcox@nasa.gov)